J. Math. Biol. (2009) 58:261–283
DOI 10.1007/s00285-008-0172-4

Mathematical Biology

From single cells to tissue architecture—a bottom-up approach to modelling the spatio-temporal organisation of complex multi-cellular systems

J. Galle · M. Hoffmann · G. Aust

Received: 17 August 2007 / Revised: 21 February 2008 / Published online: 2 April 2008

Abstract Collective phenomena in multi-cellular assemblies can be approached on different levels of complexity. Here, we discuss a number of mathematical models which consider the dynamics of each individual cell, so-called agent-based or individual-based models (IBMs). As a special feature, these models allow to account for intracellular decision processes which are triggered by biomechanical cell–cell or cell–matrix interactions. We discuss their impact on the growth and homeostasis of multi-cellular systems as simulated by lattice-free models. Our results demonstrate that cell polarisation subsequent to cell–cell contact formation can be a source of stability in epithelial monolayers. Stroma contact-dependent regulation of tumour cell proliferation and migration is shown to result in invasion dynamics in accordance with the migrating cancer stem cell hypothesis. However, we demonstrate that different regulation mechanisms can equally well comply with present experimental results. Thus, we suggest a panel of experimental studies for the in-depth validation of the model assumptions.

Keywords Individual cell-based model · Epithelial monolayer · Tumour invasion · Cancer stem cell

Mathematics Subject Classification (2000) 37N25 · 92C15 · 92C37 · 92C10 · 92C17

Electronic supplementary material The online version of this article (doi:10.1007/s00285-008-0172-4) contains supplementary material, which is available to authorized users.

J. Galle (✉) · M. Hoffmann
Interdisciplinary Center for Bioinformatics, University Leipzig, Leipzig, Germany
e-mail: galle@izbi.uni-leipzig.de

G. Aust
Centre of Surgery, Research Laboratories, University Leipzig, Leipzig, Germany

1 Introduction

Recently, increasing attention has been paid to questions on how cells and cell populations physically interact with their micro-environment. Cells are able to detect shape and stress changes within their micro-environment by sensing their own extension or compression. They couple these changes to processes such as proliferation, differentiation, and apoptosis [1–3]. Hence, basic effects of tissue organisation can directly be attributed to cell contact formation and release between individual cells and their micro-environment.

Individual-based models (IBMs) provide natural candidates for modelling the growth and pattern formation of large multi-cellular systems since they tie cellular properties to the macroscopic behaviour on the population level. They allow for an efficient simulation and permit not only analysing large cell populations but also investigating their behaviour on large time scales. Consequently, IBMs enable approaches to cell differentiation and maturation during morphogenesis and tissue formation [4–6].

A number of different IBMs of cell populations have been studied so far: (i) cellular automaton models, where each cell is represented by either a single lattice site or many lattice sites [7–11] and (ii) lattice-free models, in which cells are modelled either as Voronoi polyhedrons [5,12–14] or as deformable particles [15–20]. While for lattice-based models it is difficult to directly relate experimentally accessible quantities to the model parameters, lattice-free models open up the possibility of quantitative modelling.

Applying 3D lattice-free IBMs we have recently demonstrated that quantities like the strength of the cell–substrate anchorage have a significant impact on the morphology of cell populations and, moreover, that even the efficacy of intracellular regulation mechanisms may sensitively depend on such quantities [15]. Basic intracellular regulation mechanisms were introduced into IBMs controlling cell proliferation, apoptosis, and migration on base of cellular contact interactions. Since fundamental growth scenarios of multi-cellular systems can already be described on that level, recently such approaches were applied to a number of diverse cellular systems like epidermis [21], liver [22], lymph node [23], and colorectal tumour [24].

Regardless of this progress, active cell behaviour may be undervalued in current IBMs. Even a simple process like cell spreading on a flat substrate is not a passive act balancing adhesive and repulsive forces. Spreading encompasses a substrate sensitive, active reorganisation of the cytoskeleton, which is considered to be the pivotal process [25]. A fortiori, the complex reorganisation processes during cell migration are specifically adapted to the local environment [26,27]. Moreover, cell transformations, like the epithelial–mesenchymal transformation (EMT; [28]), induce simultaneous changes in migratory, proliferative, and apoptotic behaviour. Thus, IBMs should carefully account for (i) biomechanical parameters as targets of active regulation and (ii) regulatory interdependencies between migration, proliferation, and apoptosis.

In the present manuscript we focus on a biomechanical lattice-free IBM approach to multi-cellular growth processes previously published by us [15,24]. We start with introducing the basic model (Sect. 2) and a panel of partly novel contact-dependent regulation mechanisms (Sect. 3). Subsequently, we apply the advanced model and discuss the potential impact of these regulation mechanisms on different cellular systems

(Sect. 4). In the first application, we study intracellular feedback on cell contact formation and its impact on epithelial monolayer growth and homeostasis. In the second application, we analyse interdependencies between the regulation of tumour cell migration and proliferation with an emphasis on cancer stem cells. We suggest experiments for both applications in order to test our predictions.

2 Basic model

Computer models of cell population kinetics were already introduced in the 1960s (e.g. [29]). These early models based on data on proliferation and apoptosis of cell populations only. They ignored that cells are spatially extended objects and that their interactions with the environment determine their fates, i.e. determine whether they migrate, proliferate, differentiate, or undergo apoptosis [30]. Although of molecular origin, biomechanical properties of single cells can be characterised by a few effective parameters [31–35]. IBMs permit to take these biomechanical characteristics into account [15,19,20]. In the following, we give a brief description of the basic lattice-free model introduced by Galle et al. [15] that will be applied in the present study. The parameters of the model are specified in the Appendix (Table 1). Technical details can be found in the original article.

In the model cells are represented by *elastic objects*. They are able to move and to proliferate and can form adhesive contacts to neighbour cells and matrix components. Isolated cells are represented by elastic spheres of radius R. If cells become adherent they deform by flattening at the contact area (Fig. 1). The adhesive energy is assumed to be proportional to the contact area and depends on whether cell–substrate or cell–cell contacts are formed. The deformation energy of contact formation is approximated by the Hertz model (see Appendix). The cells are assumed to be compressible. Thus, shape changes also induce changes of the actual volume of the cells (Fig. 1). The energy related to the volume changes is approximated by that of a compressed homogeneous, elastic solid. Assuming spherical cells they can relax compression by changing their radius R (Fig. 1). According to the above assumptions, the total interaction energy of cell i is a sum of three contributions:

$$W_i = W_i^A + W_i^D + W_i^K. \tag{1}$$

where W_i^A, W_i^D and W_i^K are the interaction energies for adhesion, deformation, and compression, respectively. Details are given in the Appendix. W_i depends on the distance between cell i and its neighbouring cells and the cell radii as well as the distance of cell i to the substrate. Thus, contact formation in cell aggregates equilibrates either by cell displacements or by changes of the cell radii (Fig. 1). The parameters specifying the physical interactions are the Young modulus E, the Poisson ratio ν (or alternatively, the bulk modulus K), and the average adhesion energy per unit contact area ε_c for cell–cell and ε_s for cell–substrate contact, respectively. These parameters are experimentally accessible, e.g. by different atomic force microscopy techniques [31,36].

The deterministic forces on cell i, inducing cell displacements ($\mathbf{F}_i^{\mathrm{det}}$) and changes of the radius R_i (G_i^{det}), can be calculated from the total energies. They are given by:

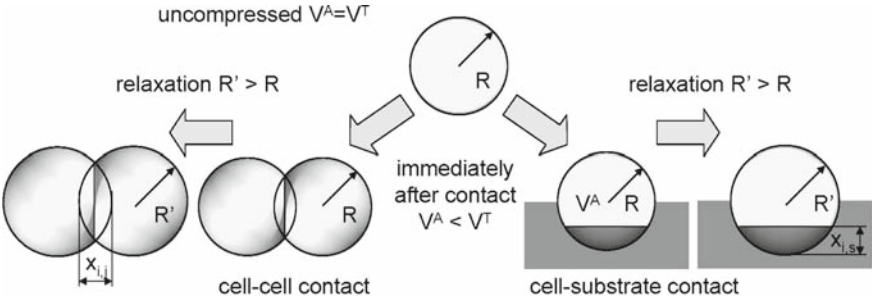

Fig. 1 Cell–cell and cell–substrate contact formation. V^A and V^T are the actual and the target cell volume, respectively. During contact formation R increases to R' in order to restore V^A to the target volume V^T. The sums of the spherical cap heights $x_{i,j}$ and $x_{i,s}$ (substrate: infinitely large sphere) are used in energy calculations

$$\mathbf{F}_i^{\mathrm{det}} = \sum_j \frac{\partial W_i}{\partial r_{i,j}} \mathbf{n}_{i,j} + \frac{\partial W_i}{\partial r_{i,s}} \mathbf{n}_{i,s} \quad \text{and} \quad G_i^{\mathrm{det}} = \frac{\partial W_i}{\partial R_i}, \tag{2}$$

respectively, with $r_{i,j} = |\mathbf{r}_{i,j}| = |\mathbf{r}_i - \mathbf{r}_j|$ and $\mathbf{r}_i$ being the position vector of cell i. In the same way $r_{i,s}$ is the distance between cell i and the substrate s. $\mathbf{n}_{i,j} = \mathbf{r}_{i,j}/|\mathbf{r}_{i,j}|$ denotes the normal vector.

The dynamics of each individual cell is modelled by *Langevin equations* applied for a friction dominated regime:

$$\mathbf{F}_i^{\mathrm{fr}} = \mathbf{F}_i^{\mathrm{det}} + \mathbf{F}_i^{\mathrm{st}} \quad \text{and} \quad G_i^{\mathrm{fr}} = G_i^{\mathrm{det}} + G_i^{\mathrm{st}}. \tag{3}$$

Thus, in the absence of an external stimulus the cells perform a random migration stimulated by a stochastic force $\mathbf{F}^{\mathrm{st}}$ with zero mean and delta-correlated autocorrelation function. Random fluctuations of the radius are generated by an analogous stochastic force G^{st}. There are different types of friction forces $\mathbf{F}^{\mathrm{fr}}(G^{\mathrm{fr}})$. While those regarding cell–medium, cell–cell, and cell–substrate friction are relevant for cell displacements, another type refers to volume changes of the cells. Cell–cell and cell–substrate friction are assumed to be proportional to the area of the contacts formed, with μ_c and μ_s being the respective factors of proportionality (see Table 1). The parameters specifying these friction forces were estimated, e.g. from cell sorting experiments [37].

Modelling *cell proliferation* a two-phase cell cycle is assumed. During the interphase, a cell doubles is target volume V^T by stochastic increments. This growth process results in an approximately Γ-distributed growth time τ of the cells. Identifying this time with the doubling time of cell populations, it can easily be measured in vitro. During the mitotic phase, a cell divides into two daughter cells of equal target volume V_0. The orientation of cell division is set to be perpendicular to the direction of the maximum force exerted on the dividing cell.

It was demonstrated that neither details of the assumptions regarding cell shape and cell division mechanisms nor assumptions about the precise shape of the interaction forces between cells significantly affects the growth behaviour of populations on long time scales [17,38,39].

3 Contact-dependent regulation mechanisms

As a special feature, IBMs allow to account for intracellular control and regulation processes triggered by cell–cell or cell–matrix interactions. In the following, we introduce IBM representations of contact-dependent regulation mechanisms regarding (I) cell proliferation, (II) apoptosis, and (III) migration, which will be applied in Sect. 4. We use the roman indices I–III to specify the fate regulated by a mechanism. Additionally, a novel shape adaptation mechanism is introduced. An overview is given in BOX1. While the mechanisms model the behaviour of epithelial cells, they may also represent regulation in other cell systems.

3.1 Cell–substrate contact-dependent regulation

The pioneering work of Ingber et al. [30] on cells cultured on micro-patterned substrates demonstrated the cell distortion-dependent mechanical signal processing and integration, causing switches between growth, differentiation, and apoptosis. The authors found that nearly all processes contributing to tissue organisation can be affected by changes of the cell shape according to substrate structure and rigidity.

In epithelial cell populations two anchorage-dependent, i.e. cell–substrate contact-dependent regulation processes are fundamental: the regulation of proliferation and the regulation of apoptosis (anoikis). Cells form adhesive contacts to the substrate through interactions employing a large variety of cell adhesion molecules [40]. Thereby, epithelia were shown to require specific basement membrane for proliferation control [41] and for suppression of apoptosis [42]. However, the key trigger for both processes was shown to be cell shape, i.e. simple epithelial cells do not proliferate and survive without a sufficiently large contact area to the substrate that allows them generating cytoskeletal tension [30]. Consistently, regulators of cytoskeleton contractility can knock-down this type of regulation [43]. In a former study [15] we introduced cell–substrate contact-dependent regulation mechanisms into the basic IBM assuming:

SI *A cell cannot proliferate and enters a quiescent state if its cell–substrate contact area* A_s *is smaller than a threshold value* A_{SI}.
SII *A cell undergoes anchorage dependent apoptosis (anoikis) with a defined rate* r_{as} *if its cell–substrate contact area* A_s *is smaller than a threshold value* A_{SII}.

Throughout this study we assume: $A_{SI} \geq A_{SII}$. Although cell spreading and migration share common features, their interdependencies are not fully understood. Cell–substrate adhesion, which is crucial for the generation of traction forces, has also been implicated in protrusion formation [44]. We do not consider a cell–substrate contact-dependent regulation of migration.

3.2 Cell–cell and cell–matrix contact-dependent regulation

Functional regulation as in multi-layered epithelia or regulatory dysfunction as in cancer can enable epithelial cells to thrive without basement membrane contact. Under these conditions cell behaviour depends on cell–cell and cell–matrix contacts. The cell

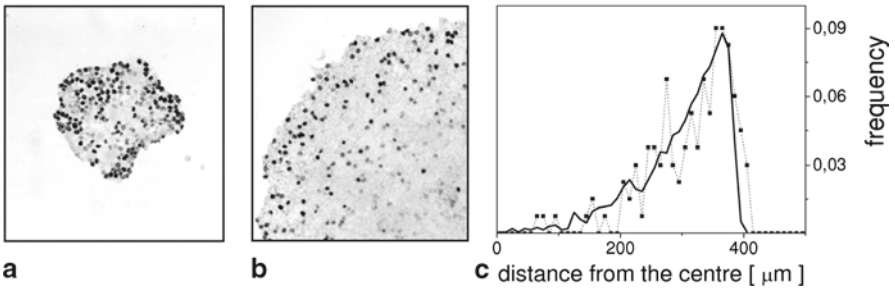

Fig. 2 Contact inhibition of growth in tumour cell populations in vitro. We analysed the proliferation activity of cancer cell lines by standard BrdU staining. **a,b** BrdU staining of HCT116 cell populations growing under standard culture conditions for **a** 7 days, **b** 13 days (selected part). **c** Radial distribution of BrdU positive cells in the colony shown in **b**. *Symbols*: experimental results, *solid line*: simulation results on HCT116 cells (please compare Fig. 4)

or matrix type to which the cells form these contacts affects their fate. While evident for functional tissue, this was demonstrated experimentally also for tumours [45,46]. Within a previous study on tumour invasion we introduced IBM representations of cell–cell and cell–matrix contact-dependent regulation mechanisms of apoptosis and migration [24]. In the present study we additionally consider regulation of proliferation assuming that:

CI–CIII: *The number of contacts N_x formed to a specific cell type x acts as a trigger for reversible regulation of* (**CI**) *proliferation*, (**CII**) *apoptosis, and* (**CIII**) *migration*.

These mechanisms may be understood as analogous to the cell–substrate contact-dependent regulation mechanism described above. They will be specified in the applications in Sect. 4.

3.3 Density-dependent regulation

Over time, proliferation unavoidably induces high density regions in cell populations. In anchorage dependent confluent monolayers (see Fig. 2 and [47]) as well as in anchorage independent cell spheroids [48] increasing cell density was shown to stop proliferation, i.e. the cells enter a quiescent state. In a multi-particle system increasing density enlarges the inter-particle contact area and increases particle compression.

Before the onset of active cell reaction (see below), the same can be assumed for multi-cellular systems. Currently, it is unknown, which effects trigger the observed proliferation stop. Based on the results of Helmlinger et al. [48] on spheroids we introduced in [15] a related regulation mechanism assuming that:

PI *A cell cannot start proliferation as long as it is compressed below a threshold volume V_P.*

Density-dependent apoptosis is known for different cell systems, e.g. for in vitro cultures of fibroblasts [49]. Both, density- and anchorage (SII)-dependent apoptosis were suggested to be regulated by common mechanisms converging at the level of Bcl-2 activation as a major apoptosis-suppressive mechanism [50]. Moreover, epithelial

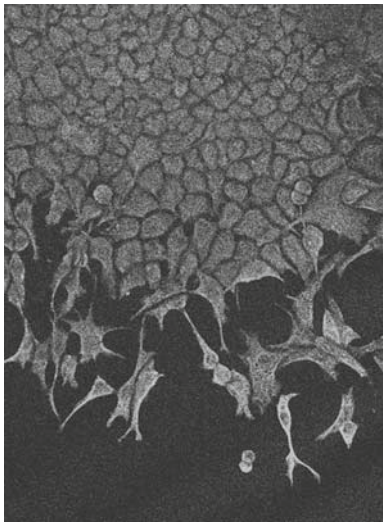

Fig. 3 Cell density gradient in colonies grown in vitro. Periphery of a HCT116 colony growing under standard culture conditions. We used fluorescence immunostaining to visualize the intermediate filaments. Obviously, the bulk of the colony is most densely packed

cell–cell contact was shown to affect cell migration confining the protrusive cell activity to regions free of contact [44].

Accordingly, within this study we additionally assume that:

PII *A cell may undergo density-dependent apoptosis with a rate* r_{ap} *in parallel to density-dependent contact inhibition of proliferation* (PI).
PIII *Quiescent cells may undergo density-dependent inhibition of migration, which is modelled by switching-off the stochastic force* F_{st}. *As an option cells may perform an orientation-biased migration* (*e.g. at the population boundary, see below*).

3.4 Cytoskeletal reorganisation

At the periphery of many cell populations growing in vitro a cell density gradient can be detected which is accompanied by alterations of the cytoskeletal organisation. In the cancer cell colony shown in Fig. 3 isolated cells show an elongated, migratory phenotype, whereas cells confined in the colony show a compact polyhedral morphology. Among the latter, cells at the periphery spread more efficient than cells in the bulk of the colony. Such morphological changes of the cell are a result of active cytoskeletal reorganisation induced by contact formation. Thereby, cells globally control their cytoskeleton [51] and thus, each new contact formed will affect all of the other contacts. Large changes of 3D cell shapes according to contact formation were analysed by approaches that describe cell shapes either by ellipsoids [16,19] or Voronoi polyhedrons [13,21]. In these models the deformation energy of a cell depends on the degree of deformation only.

In a different approach we here assume the deformation energy of the cells to depend additionally on the type of contact formed (cell–substrate or cell–cell contact). Moreover, we assume the Young moduli to be regulated in a contact-dependent manner. Thereby, and in contrast to the above mentioned approaches, the intrinsic shape of the

cells remains spherical, independent of the contacts formed. Such an approach can directly account for certain cellular adaptation processes like active cell spreading at the periphery of a cell population. However, it does not consider the complexity of the cell shapes, shown in Fig. 3. A more detailed description of the shapes of migrating cells goes beyond the scope of the model (see also Sect. 5).

In a dense epithelial monolayer cells polarize perpendicular to the substrate. If these cells loose their cell–cell contacts, e.g. as induced by growth factors, they spread actively and often become migratory [28]. In the following, we consider a cytoskeletal reorganisation process that models aspects of epithelial polarisation as a positive feedback to cell–cell contact formation. We assume for cells with substrate contact:

A0 *Bulk cells pile-up promoting cell–cell contact formation while isolated cells actively spread and promote cell–substrate contacts.*

This behaviour is modelled assuming the (effective) Young modulus for promoted deformations E_p to be smaller than the respective modulus E in a passive scenario. At the same time the modulus of non-promoted deformation is assumed to be larger than E, enforcing the intended shape changes. The deviation from E is denoted by ΔE. We assume $\Delta E_s = (-2)\Delta E_c$, with s and c indicating the formation of cell–substrate and cell–cell contacts, respectively. We define a threshold value for the cell–cell contact area A_A, above which cells are considered to be bulk cells. The bulk modulus K of the cells is assumed to be unaffected.

Box1: Overview of contact-dependent regulation mechanisms. SI–SIII: cell–substrate contact-dependent regulation. CI–CIII: cell–cell and cell–matrix contact-dependent regulation. PI–PIII: cell compression (respective density) dependent regulation. A0: surface adaptation through cytoskeletal reorganisation. A_S and A_C denote the actual cell–substrate and the cell–cell contact area, respectively. V_A is the actual cell volume and N_x the number of cell contacts to cells of type x. A_{SI}, A_{SII}, A_A, V_P, and N_C denote the threshold values described in the text. $\mathrm{V}(A_c = A_A)$ denotes the volume of a cell that forms a contact area A_A to neighbouring cells.

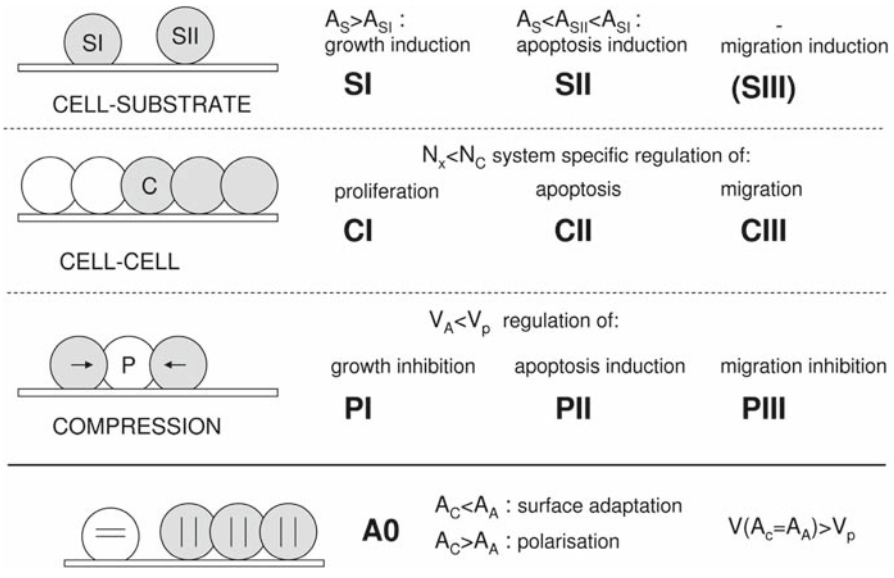

4 Applications

In the following, we discuss the organisation of two biological systems which are well suited for being modelled on an IBM level: (Sect. 4.1) the in vitro expansion of cell populations and (Sect. 4.2) microscopic collective tumour cell invasion. In both cases nutrient and oxygen supply is assumed to be abundant. The first application broaches the issue of active surface adaptation, while the second focuses on interrelations between different regulation mechanisms. In each application only a subset of the regulation mechanisms introduced in Sect. 3 is considered.

4.1 On the origin of quiescence in cell populations

First, we discuss two hypotheses about growth regulation of cell populations in vitro. They differ with respect to their assumption about the origin of quiescence. Let us consider a cell colony growing in a Petri dish from a single cell. The Petri dish is modelled as a hard sphere with infinite radius to which the cells can adhere (Fig. 1).

Scenario R1 *If the initial cell spreads sufficiently* ($A_s > A_{SI} > A_{SII}$) *it starts proliferating. The daughter cells have comparable properties and so they continue proliferation. During the growth of the clone, cell–cell contacts form. As a result the cells in the bulk of the colony are compressed* ($V_A < V_P$) *and if they retain sufficient substrate contact* ($A_s > A_{SII}$) *they undergo a cell–cell contact mediated form of growth inhibition.*

In this scenario, regulation types SI, SII and PI are considered. The growth regulation results in biphasic growth dynamics. The initial phase, in which the cell number grows exponentially, is followed by a growth phase which is characterised by a finite width of the proliferation zone at the periphery of the colony and a constant growth velocity of its diameter. This behaviour is found for a large number of experimental cell systems in vitro (Fig. 4, [47]).

One characteristic of this scenario is the sensitivity of its growth behaviour to density-dependent growth inhibition PI [15]. Let us consider a cell colony forming a stable monolayer. Moreover, the cells may be sensitively regulated by PI, i.e. $V_P - V_0$ may be small. A small decrease of the threshold volume V_P in that system increases the spreading velocity of the colony. However, decreasing V_P even further destabilises the monolayer. Cells are pushed out of the layer and undergo anoikis (SII). Thereby, the colony spreading velocity decreases.

A knock-down of the regulation SI and SII in such a model colony leads to 3D cell growth. 3D growth patterns were also found experimentally for cell lines growing in vitro suggesting a comparable regulation scenario (Fig. 4c). However, regulation in this model requires persistent cell compression in the bulk of the colonies. This contradicts the idea of tissue homeostasis.

One might expect that the related stress would lead to apoptosis and, subsequently, to tissue relaxation or proliferation in the bulk of the colony, filling the space provided by apoptosis. Therefore, it is plausible to consider density-dependent apoptosis PII. In simulations we found that apoptosis of quiescent cells can lead to pressure relaxation

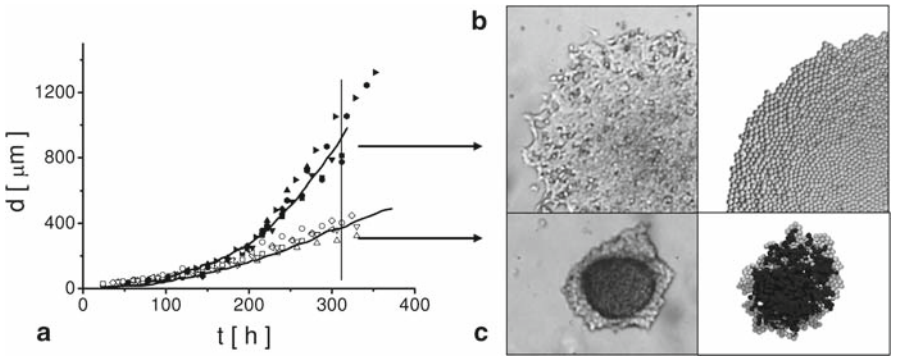

Fig. 4 Colony growth dynamics and morphology in vitro: **a** colony diameter versus time of cells of colorectal carcinoma cell lines, HCT116 (*solid symbols*) and SW480 cells (*open symbols*), growing under standard culture conditions (own results). Different symbols denote different colonies. A constant colony spreading velocity is observed after about 10 days. The *solid lines* are simulation results considering scenario R1. **b** HCT116, **c** SW480 typical colony morphology (*top views*) after 13 days of standard culture (*left*) compared to simulation results (*right*). Dark cells are cells without cell–substrate contact. The morphology ranges from a nearly perfect monolayer (HCT116) to 3D patterns. 3D patterns of SW480 cells were simulated by switching-off anchorage dependent regulation (SI, SII). For parameter sets related to 'HCT116' and 'SW480' and fitting procedures, please, see Appendix. Please refer the online version of the article for colored figure

within cell populations assuming high bulk cell motility (unpublished results). Accordingly, contact inhibition of migration PIII has to be inactive. In the following, we will consider a second scenario about the regulation of colony growth that does not require the above assumptions.

Scenario R2 *Sufficient spreading of the initial cell* ($A_s > A_{SI} > A_{SII}$) *requires an active reorganisation of its cytoskeleton. Such reorganisation (substrate adaptation,* $A_c < A_A$) *allows the cell starting proliferation. Its daughter cells have comparable properties and so they continue proliferation. If cells in the growing colony form sufficient contacts with their neighbours* ($A_c > A_A$) *they reorganize their cytoskeleton promoting further cell–cell contacts (polarisation) and, subsequently, pile up. As a result the cell-substrate contact area of these cells falls below a threshold value* ($A_s < A_{SI}$). *Thus, they undergo a cell–substrate contact mediated form of growth inhibition and enter a quiescent state.*

In this scenario the regulation mechanisms SI, SII, and A0 are considered. This type of growth regulation also leads to biphasic growth dynamics like the first scenario R1, i.e. the scenarios R1 and R2 are indistinguishable with respect to growth curves. The result is independent of whether PI is active or not (not shown). In fact, for different friction coefficients (higher coefficients in case of R1, see Appendix) two colonies regulated according to R1 and R2, respectively, can show identical expansion behaviour as demonstrated in Fig. 5a. However, the R2 scenario enables the bulk cells to relax their compression, i.e. enables tissue homeostasis without apoptosis. In the relaxed state the bulk cells do not proliferate. The proliferation zone at the periphery of the colony is formed by substrate adapted cells (Fig. 5d, e).

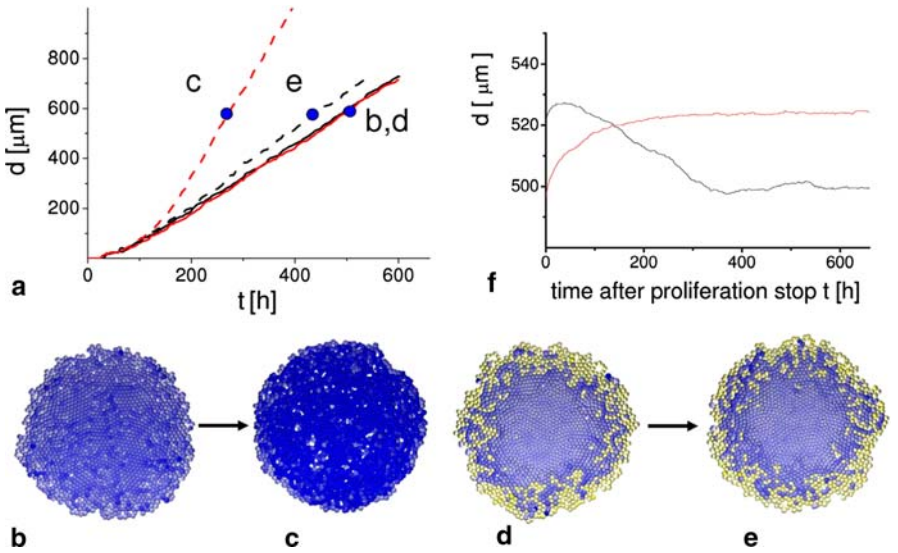

Fig. 5 Comparison of growth dynamics according to scenarios R1 and R2. **a** Colony diameter versus time. **b–e** Top views of colonies at the time points indicated in **a**. **b–e** Colour saturation indicates cell compression, substrate adapted cells (A0) are shown in *yellow*. Two colonies, regulated according to R1 (**a**: *solid red line*, **b**) and to R2 (**a**: *solid black line*, **d**) show nearly identical spreading. This is achieved by assuming different cell–substrate friction coefficients. Decreasing the threshold volume V_P from $0.99V_0$ to $0.9V_0$ in both systems, R1-regulated cells show a faster colony expansion (**a**, *dashed red line*) and large cell compression (**c**). In contrast R2-regulated cells show only marginal changes in the dynamics (**a**, *dashed black line*) and compression (**e**). **f** Relaxation dynamics of colonies with 1,000 cells after a proliferation stop. Colonies of cells regulated according to R1 (*red*) expand while colonies of *R2-regulatd* cells (*black*) contract. For parameter sets 'R1 versus R2', please, see Appendix. Please refer the online version of the article for colored figure

In both scenarios colonies completely relax if proliferation is switched-off. While those colonies regulated according to R1 expand, R2-regulation leads to contraction (Fig. 5f). We suggest testing this behaviour in vitro by switching-off proliferation, e.g. using a DNA polymerase inhibitor or an alkylating agent [52]. The contraction phenomena observed for cell monolayers by Nelson et al. [53] confining the growth of cell colonies to micro-fabricated adherent islands suggests R2-regulation for epithelial and fibroblast colonies.

In case the cytoskeletal reorganisation A0 is more sensitive to cell density than the cell–cell contact-mediated growth inhibition PI, as assumed in our simulations ($V(A_A) > V_P$, BOX1), R2-regulated colony spreading becomes insensitive to PI regulation. Under this assumption even a strong decrease of V_P, i.e. a *quasi*-loss of PI-regulation, has only a marginal impact on spreading. In remarkable contrast to scenario R1, and regardless of the lower cell–substrate friction assumed in R2 compared to R1, the spreading velocity changes only slightly and cells are not pushed out of the monolayer bulk because they are not subjected to compression (Fig. 5b–e). As a further consequence, switching-off the anchorage dependent proliferation stop SI in a colony leads to hyper-proliferation controlled by PI-regulation (not shown). This kind of behaviour could be studied experimentally, e.g. by altering RhoA/ROCK signalling [43] or c-Myc expression [54] in spreading cell colonies.

Surprisingly, we observed that for R2-regulation an increase of the adhesion constant ε_s can result in an increased colony spreading velocity (not shown). The more adhesive cells at the periphery stronger resist the pushing forces of the neighbouring cells and are forced to form larger cell–cell contacts. Increased cell–cell contacts switch on cytoskeletal reorganisation A0 near the border of the colony and decrease the width of the zone containing substrate adapted cells. As a result, the cell–substrate friction forces, being proportional to the contact area, are reduced allowing a faster spreading of the colonies.

These results suggest a reconsideration of the *origin and possible regulation of cellular friction*. In our opinion, the cell–cell and cell–substrate friction constants are determined by the limited turnover of the adhesion structures generated by the cells, e.g. by the limited turnover of focal adhesions. Thus, each change in turnover would change the friction constants. In this way, an enhanced focal adhesion turnover induced, e.g. by increased myosin light chain kinase activity [55] should result in a reduced cell–substrate friction and thus, faster colony spreading. This could be tested experimentally.

4.2 On interdependencies between tumour cell migration and proliferation

Scattered cells at the tumour front represent a morphological feature often clinically related to increased invasion and metastasis and thus, to poor prognosis. These cells have characteristic gene and protein expression profiles [45,46,56] distinct from cells located in the tumour centre (bulk cells). It is a challenge to understand whether and how these scattered cells contribute to tumour invasion. In this context, we will discuss IBM approaches to collective tumour invasion. After a short overview over published results on proteolytic tumour invasion considering regulated apoptosis and migration [24] we focus on novel results on the interdependencies between regulation of tumour cell migration and proliferation.

While single tumour cells may penetrate the surrounding tissue without substantially affecting its composition [57,58], collective tumour invasion requires sustained stroma decomposition. Mere tissue deformation by the tumour would generate large within-tissue pressure that would in turn stop tumour proliferation via the density-dependent growth inhibition PI (compare Fig. 6). Therefore, IBMs and also continuum models of tumour invasion typically consider either apoptosis or proteolysis [24,59]. Invasion based on non-specific apoptosis of stroma and tumour cells leads to competition between tumour and stroma cells for the space generated by apoptosis throughout the tissue. Hence, it involves long range tissue reorganisation. Proteolytic invasion acts locally at the invasion front. Both, apoptosis and proteolysis induced invasion can be shown to require a decreased sensitivity of the tumour cells to density-dependent growth inhibition (PI, unpublished results).

In a recent study [24] we have introduced a basic IBM approach to *proteolytic tumour invasion*. A population of stroma cells, representing both stroma cells and matrix, is expanded until it fills a closed box generating a persistent within-tissue pressure. This pressure keeps the stroma cells quiescent. Subsequently, an initial tumour clone is generated by selecting a few cells ($\sim$30) at the centre of the box

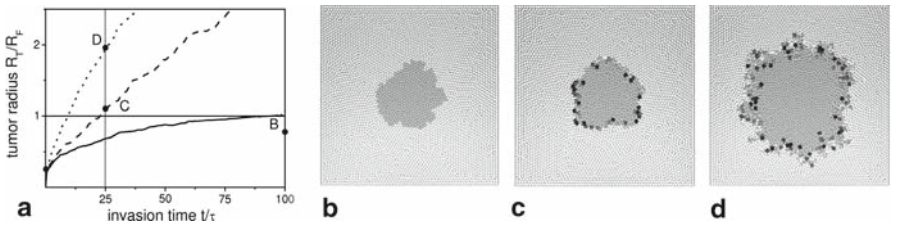

Fig. 6 Tumour invasion dynamics. **a** Tumour radius R_T versus time t for tumour expansion ($r_d = 0$, CIII: off, *solid line*), proteolytic invasion ($r_d = 0.2$/day, CIII: off, *dashed line*), proteolytic invasion with activated orientation-biased migration ($r_d = 0.2$/day, CIII: on, *dotted line*). **b–d** Top views of growing tumours at time points indicated in **a**. *Dark grey cells* are tumour cells, *black cells* being tumour cells with immanent cell division. R_F denotes the finite tumour radius approached without any proteolytic activity. For the parameter set please see Appendix

and decreasing their sensitivity to contact inhibition of growth. These tumour cells are assumed to degrade the surrounding stroma cells with a rate r_d (0.2/day) per cell–cell contact, i.e. we assume the cells to be proteolytically active. This proteolytic activity of the tumour cells ensures a persistent invasion. After a non-linear expansion phase the tumour invasion radius grows with an almost constant velocity (Fig. 6). This velocity is directly proportional to the degradation rate r_d and the total number of tumour-stroma cell contacts.

Full 3D morphology screening of the simulated tumours would require a system size of about $10^5 - 10^6$ cells [17] which can hardly be managed at the present level of detail. However, monolayer variants conserve basic features of 3D growth dynamics. In fact, these systems may describe the expansion of a tumour cell clone in, e.g. a fibroblast cell layer in vitro. In the following, we present selected simulation results on such monolayer systems.

Modelling regulated tumour apoptosis and migration In Ref. [24] we have already analysed the impact of tumour cell apoptosis and activated migration at the tumour front on the invasion dynamics. For this purpose we introduced regulation schemes of type CII and CIII, respectively. We introduced a threshold number N_C of tumour cell neighbours below which the parameter set of the tumour cells changes (i.e. $N_{(x=T)}$: number of tumour cell neighbours). Assuming that stroma contact promotes migration, we considered two changes: (i) an increase of the amplitude of the stochastic force $\mathbf{F}_{st}$ and (ii) an orientation-bias of this force. According to the model each migration step at the front points out of the tumour into the stroma. Moreover, we assumed that stroma contact may induce tumour cell apoptosis with a rate equal to the proteolytic degradation rate of stroma r_d.

While activated random migration and apoptosis were found to have only marginal effects on the invasion dynamics, an activated and orientation-biased migration significantly increases the proteolytic tumour surface and consequently speeds up invasion (Fig. 6a, d). The migratory activated tumour cells scatter at the invasion front. Thus, the model shows phenomenological features of an EMT at the invasion front often observed during tumour invasion and found to be crucial for malignant progression [28,60]. Our results turned out to be independent of the choice of the threshold num-

ber N_C. Henceforth, we consider N_C to be equal to half the number of all cell–cell contacts N_0 realised by a cell.

Modelling regulated tumour proliferation Tumours often show distinct sub-areas of extensive proliferation, quiescence, differentiation, and EMT. These phenomena can be explained by considering tumour stem cells [61]. A common paradigm regarding stem cell properties is the pedigree concept, which treats 'stemness' as an intrinsic cellular property [62]. However, experimental findings dealing with tissue plasticity phenomena [63,64] have indicated that cell–cell and cell–substrate interactions can influence stem cell development in a variety of ways leading to novel stem cell concepts that assigns the interaction between cells and their growth environment a greater emphasis [65,66]. These concepts do not exclude certain preferred trends in the differentiation sequence, but they enable reversible developments for individual cells, allowing the system to flexibly react to changing demands. In the deduced non-spatial models, stem cell self-renewal, heterogeneity, and lineage specification are results of self-organisation processes [67]. A simple approach to spatially organised population heterogeneity was suggested by Stockholm et al. [68].

In the following, we discuss two hypotheses related to cancer stem cell organisation. As a reference, we consider the invasion model with environmentally regulated orientation-biased migration (CIII, Fig. 6d).

Scenario R3 *Tumour cell proliferation is extrinsically regulated by the tumour environment. Tumour cells in the bulk* ($N_T > N_C$) *are capable of proliferation depending on compression* ($V_A > V_P$). *In contrast, tumour cells which are exposed to stroma* ($N_T < N_C$) *enter a quiescent state independent of their compression. This regulation is reversible*.

The above scenario considers the regulation mechanisms PI and CI. In a monolayer the mechanisms SI and SII may be considered as well. Although stem cells are not explicitly defined in this scenario, the model can be linked to the tissue stem cell model of Loeffler and Roeder [65]. This model assumes two different stem cell environments: a growth and a niche environment. In the growth environment the cells proliferate and loose stem cell properties, while in the niche environment they are quiescent and re-gain stem cell properties. Here, we assume stroma to be a cancer stem cell niche. Accordingly, tumour cells in contact with stroma enter a stem cell state. This is motivated by the observed stem cell-like expression profile of scattered tumour cells [45,46,61] and is in agreement with experiments demonstrating a low proliferation activity of scattered cells at the tumour front [69]. Tumour cells of the bulk can proliferate, i.e. the tumour bulk represents the growth environment. Accordingly, bulk cells are assumed to become reversibly differentiated.

We started the simulation with identical cells. Subsequently, these cells were subjected to environmental regulation of proliferation CI and migration CIII. The regulation of proliferation was found to have only a minor effect on the invasion velocity and tumour morphology compared to the reference system (Fig. 6d). Migratory activated cells show a reduced proliferation rate, i.e. only those of them proliferate that started cycling before becoming migratory (Fig. 7a–c). Thus, stem cells are migratory activated and mostly quiescent in this model, as suggested by the migratory cancer

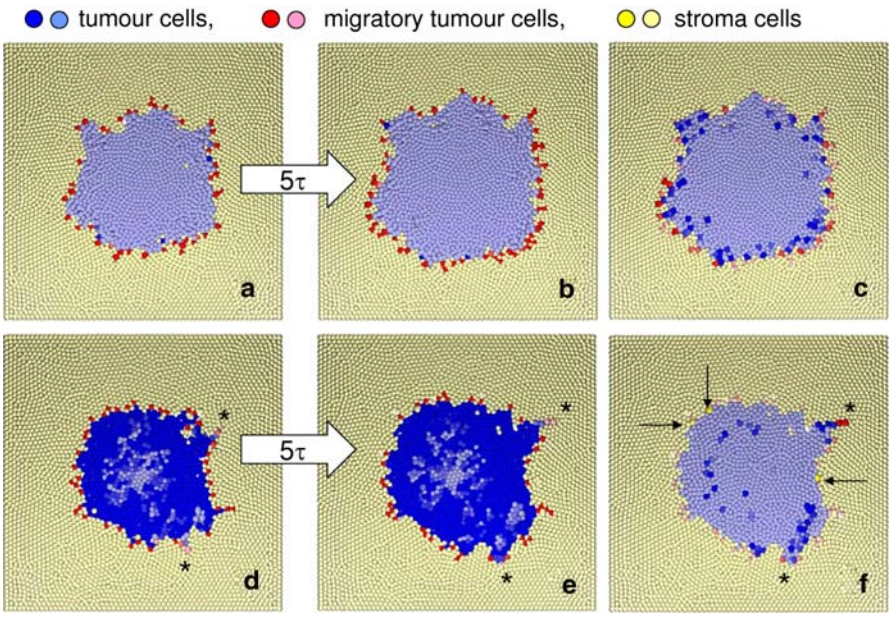

Fig. 7 Cancer stem cell organisation. Top views on tumours after an invasion time of **a, d**: 25 and **b, c, e, f**: 30τ (τ: cell growth time). Colour saturation indicates **a, b** stem cells, **d, e** differentiated cells, **c, f** immanent cell division. **a–c** Environmentally regulated proliferation according to the plasticity scenario R3: the migratory cells at the tumour front are considered to be quiescent stem cells. **d–f** Intrinsically regulated proliferation according to the pedigree scenario R4: most of the stem cells are located in the tumour bulk. Stem cells located at the tumour periphery stay there and induce fast invasion (*, **d, e, f**). Typically, proliferating stroma cells are found at the tumour front (*arrows*). For parameter sets 'R3 versus R4', please, see Appendix

stem cell hypothesis [61]. In the following we compare the above results (R3) to a pedigree scenario (R4).

Scenario R4 *Tumour cell proliferation is intrinsically regulated according to a pedigree model. Tumour stem cells divide asymmetrically generating a stem cell and a transient amplifying cell. Transient amplifying cells perform a limited number of symmetric cell divisions* ($N=4$) *generating new transient amplifying cells before entering a non-proliferative differentiated state. With a small probability* (*10%*) *the tumour stem cells divide symmetrically, thereby expanding the stem cell pool.*

In the pedigree-type simulations the initial tumour is assumed to consist of stem cells only. During invasion most of them become confined in the tumour bulk, only a few localising at the invasion front (Fig. 7d, e). This localisation pattern leads to specific invasion dynamics and heterogeneity. Expansion of stem cell clones confined within the tumour bulk requires that proteolytic activity at the invasion front enables relaxation in the bulk. Since relaxation proceeds from the tumour front, bulk stem cells become more and more quiescent with increasing distance from the front. Simultaneously, stroma cells start proliferation in front of the tumour filling the space generated by the proteolytic activity of the tumour cells (Fig. 7f). Consequently, the invasion

slows down. In contrast, stem cells which are located at the invasion front and are therefore migratory activated bear rapidly expanding clones (Fig. 7f). The local invasion dynamics is comparable to that observed assuming no regulation of the proliferation at all, as in the reference case. The migratory stem cells at the front proliferate. Thus, a clear difference between the invasion dynamics according to R3 and R4 can be stated: only scenario R3 complies with the migratory cancer stem cell hypothesis.

Assuming a stroma-mediated induction of tumour cell apoptosis at the front (CII) the few migratory stem cells of the pedigree model R4 would be targeted by this mechanism and vanish. Thus, the tumour cell apoptosis would have a significant tumour suppressor effect under these assumptions. In contrast, in the plasticity scenario R3 tumour cell apoptosis would have only marginal effects because stem cells are abundant at the tumour front. Moreover, let us consider stem cell-specific chemo-attractants in the tumour stroma, e.g. specific chemokines secreted by inflammatory cells within the stroma or nearby endothelial cells [70]. These attractants would recruit stem cells to the tumour periphery. Within the plasticity scenario R3 collective tumour invasion speed is insensitive to such long range signalling. In contrast, in the pedigree scenario R4, migratory activation of tumour cells at the invasion front displays its invasive potential only in presence of such long range signalling. For better understanding of cancer stem cell organisation we suggest developing sophisticated in vitro models of tumour invasion that allow testing such predictions under controlled conditions. The observed persistence of stem cell properties in cancer cell lines [71] may facilitate such investigations.

5 Discussion

Recently, contact-dependent regulation mechanisms were demonstrated to be capable of explaining fundamental properties of the spatio-temporal organisation of very different multi-cellular systems. Nevertheless, many questions regarding biomechanical feedback mechanisms and the interdependencies between the regulation of migration, proliferation, and apoptosis still remain open. Within an IBM approach we have shown that intracellular feedback on cell contact formation can be a source of epithelial monolayer stability and tissue homeostasis, and that cancer stem cell properties may strongly affect the dynamics of tumour invasion.

The basic IBM described in this study has some clear limitations. In particular, this regards the description of *cell shape and cell migration*. Both properties are intimately linked in real systems. As an example, while a round cell shape of epithelial cells is often linked to amoeboid migration, elongated cell shapes are observed when epithelial cells switch to fibroblast-like migration [26]. Assuming a basically spherical cell shape, the present model cannot account for these details. However, are such details essential?

Under certain conditions they are! For instance Beyer and Meyer-Hermann [23] demonstrated that fast-migrating cells require more detailed models of cell migration to account for their experimentally observed velocity distribution in dense tissues. Moreover, in dense tissues a cell shape description by Voronoi polyhedrons has clear advantages, avoiding multi-particle volume overlaps [12]. Here, we introduced a model

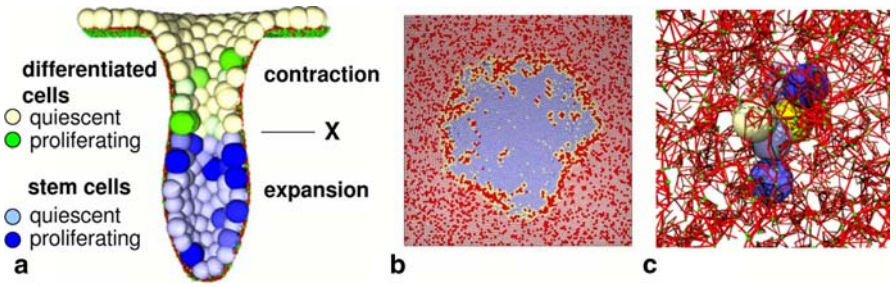

Fig. 8 Model extensions. **a** IBM of an intestinal crypt. The basement membrane (*red*) is modelled as cross-linked (*small green dots*) random polymer network. Cell turnover is driven by the expansion of stem cells (*blue*) and by contraction of differentiated cells (*yellow*). Stem cells start differentiation crossing a defined crypt position *X* (cells during their last proliferation cycle: *green*). **b,c** Tumour stroma representation in IBMs. **b** Extended version of the basic tumour invasion model assuming that the tumour cells (*blue*, activated: *yellow*) can degrade only a part of the stroma: degradable component (*light red*), non-degradable component (*dark red*). **c** Future extensions may consider explicit representations of collagen networks (*red*). Please refer the online version of the article for colored figure

of cytoskeletal reorganisation describing aspects of epithelial cell polarisation in monolayers. An extension of this idea to collective cell shape changes in 3D as observed, e.g. during chondrogenesis [72] would also require a more detailed description. Further examples may be IBMs of contact guidance of cells [73]. In order to tackle these problems efficiently one may favour modularly organised IBMs that allow specifying the intended level of detail. Recently, modelling platforms like CompuCell [74] have encouraged such ideas. However, focussed models have complementary potential for explaining specific cell biological phenomena.

The two applications of the present study analyse in vitro growth of epithelial cell populations and collective invasion dynamics of carcinoma, respectively. Thus, they both account for cellular organisation in a *strange, non-native environment*. Clearly, the organisation of functional tissue cannot be fully understood without considering its integration into an organism. We suggest to start with a proper representation of specific interfaces. Regarding epithelial tissues, modelling basement membrane is an issue. Compared to cells, these polymer networks, although remodelled permanently, are very stiff, supporting tissue integrity. Moreover, their local composition was shown to affect cell fates [75]. Recently, we started modelling these structures using random networks (Fig. 8a). Simulating fundamental biological processes like cleft formation [41] and crypt fission [76] it is a challenge to account for basement membrane remodelling regarding both structure and composition. Approaching tumour invasion by IBMs a more sophisticated representation of the tumour stroma is a further issue of model improvement. This may include multi-component stroma (Fig. 8b) and explicit representations of the collagen matrix of connective tissue (Fig. 8c).

In the present manuscript we focused on IBMs of microscopically sized systems. Modelling *macroscopic tissue* requires accounting for nutrient and oxygen supply. In order to achieve this requirement a number of hybrid models were introduced combining different types of IBMs with differential equation models describing the molecule transport through the tissue [8,17]. Other possible extensions of IBMs are,

e.g. explicit representations of intracellular regulation networks, starting with simple transcription factor networks [77], and models of autocrine cell communication [78]. As pointed out by Roose et al. [79] the comprehensive validation of these complex theoretical models will require, beside the collaboration with experimentalist, also the interdisciplinary collaboration between theoreticians themselves.

6 Conclusions

IBMs are capable of explaining fundamental properties of the spatio-temporal organisation of very different multi-cellular systems. However, as demonstrated in this study, different model assumptions can equally well comply with present experimental results. Thus, in order to develop reliable quantitative IBMs additional experimental studies are required for identifying the actual nature of contact-dependent regulation.

For a better understanding of contact-dependent cell polarisation in epithelial monolayers we suggest analysing the spatio-temporal organisation of such monolayers while manipulating cell proliferation either by arresting cells in the cycle or by molecularly interfering with the anchorage dependent proliferation control. Moreover, manipulating the focal adhesion turnover should provide essential information on the relationship between cell adhesion and friction which in turn impacts cell contact formation. In order to identify contact-dependent regulation of tumour cell proliferation in carcinoma future experiments should quantify the impact of stroma-induced tumour cell apoptosis and cancer stem cell recruitment on invasion dynamics.

Acknowledgments We thank Dirk Drasdo for fruitful discussion and useful hints. This study was supported by a joint grant from the German Research Council (DFG; AU 132/3-1). J.G. was supported by DFG-grant BIZ-6 1/1; M.H. by BMBF-grant 0313836.

Appendix

The total interaction energy of a cell comprises the energies for adhesion, deformation, and compression. In the following, the methods for calculating these contributions are explained in more detail.

We study dynamics on a time scale that is large compared to that of receptor–ligand binding. Accordingly, we can neglect the fluctuations in the number of binding sites during the formation and release of cell contacts and approximate both the adhesive cell–cell and cell–substrate interaction energy for cell i by:

$$W_i^A = \varepsilon_c \sum_{j \neq i} A_{i,j}^C + \varepsilon_s A_{i,s}^C \,, \tag{A.1}$$

where ε_c and ε_s denote the average adhesion energy per unit contact area between cells and a cell and the substrate, respectively. The actual contact areas between cell i and cell j and substrate s are denoted by $A_{i,j}^C$ and $A_{i,s}^C$, respectively. We use the circular area representing the base of the overlapping spherical caps for the contact areas (Fig. 1).

Our model approximates cells as homogeneous, elastic spheres. We neglect shear deformations and assume that the deformation energy of cell i can be calculated according to the Hertz model:

$$W_i^D = \sum_{j \neq i} \frac{2x_{i,j}^{5/2}}{5D_{i,j}} \sqrt{\frac{R_i R_j}{R_i + R_j}} + \frac{2x_{i,s}^{5/2}}{5D_{i,s}} \sqrt{R_i}, \tag{A.2}$$

with R_i and R_j denoting the cell radii and $x_{i,j}$ ($x_{i,s}$) being the distance between cell i and cell j (cell i and substrate s). $D_{i,j}$ and D_{is} are defined through the Young moduli E_i and E_j and the Poisson ratios ν_i and ν_j of the cells:

$$D_{i,j} = \frac{3}{4}\left(\frac{1-\nu_i^2}{E_i} + \frac{1-\nu_j^2}{E_j}\right), \quad D_{i,s} = \frac{3}{4}\left(\frac{1-\nu_i^2}{E_i}\right). \tag{A.3}$$

The extent to which a cell is able to resist a compression depends on its bulk modulus K. We approximate the energy associated with changes in cell volume by:

$$W_i^K = \frac{K}{2\,V_i^T}\left(V_i^T - V_i^A\right)^2, \tag{A.4}$$

in which V_i^T is the target volume and V_i^A the actual volume of cell i. V_i^A is the volume of the sphere with radius R_i diminished by the sum of all spherical caps of this sphere overlapping with neighbouring cells and the substrate (Fig. 1).

Table 1 shows the model parameters used in the simulations presented in Figs. 2, 4–7, as well as the activity of the considered regulation mechanisms. Exceptions are the simulations regarding the basic invasion model presented in Fig. 6. In these simulations the parameter set named "R3 versus R4" was applied with the modifications described in the legend of Fig. 6 and CI not being active. All model parameters not specified in the Table were taken from [15]. In the presented simulation PII, PIII, and CII were not considered. N_0 denotes the number of all contacts of a cell to other cells. V_0 is the volume of a sphere with radius R_0 and D_0 the migration coefficient of an inactive cell [24].

Parameter setting for tumour cell lines HCT116 and SW480 cells was performed in a multi-step procedure. Values for the cell radius R_0 and the doubling time τ were taken from own cell culture measurements. All other parameters were initialised by appropriate values taken from the literature. Young modulus: ∼1 kPa [31], cell–substrate and cell–cell anchorage: 100–1,000 μNm [80], friction constant: $10^{10} - 10^{12}$ Ns/m (corresponding to high cytoplasm viscosity [37]), anoikis rate: 0.25/h [81]. The bulk modulus was set to be equal to the Young modulus corresponding to a Poisson ratio of 1/3 as suggested by Ref. [57]. Subsequently, the spreading velocity was adjusted by variation of the friction constant. The shape of the population was modified by changing the cell–substrate anchorage. Finally, the Young modulus was fixed to adjust details of the growth curves of the population radius.

Parameters for R1–R4 scenarios were not chosen with respect to a specific cell system.

Table 1 Simulation parameter

PARAMETER	Symbol	HCT116	SW480	R1 versus R2		R3 versus R4	
				R1	R2	R3	R4
radius of a free cell	R_0	7μm	7μm	8μm		5μm	
cell growth time	τ	24 h	32 h	21 h		21 h	
Young modulus	E E_p	1.5 kPa /	0.75 kPa /	2.0 kPa /	2.0 kPa 0.5 kPa	0.75 kPa /	
bulk modulus	K	1.5 kPa	0.75 kPa	2.0 kPa	2.0 kPa	0.75 kPa	
cell-substrate anchorage	E_s	600 μN/m	50 μN/m	600 μN/m		600 μN/m	
cell-cell anchorage	E_c	200 μN/m	200 μN/m	200 μN/m		200 μN/m	
friction constant	$\mu_s = \mu_c$	$3x10^{10}$ Ns/m³	$3x10^{11}$ Ns/m³	$6x10^{11}$ Ns/m³	$3x10^{11}$ Ns/m³	$3x10^{11}$ Ns/m³	
SI threshold area	A_{SI}	on >0 μm²	off /	on >0 μm²	on 160 μm²	on >0 μm²	
SII threshold area anoikis rate	A_{SII} w_{as}	on >0 μm² 0.25/h	off / /	on >0 μm² 1.00/h		on >0 μm² 0.25/h	
PI threshold volume	V_p	on $0.99V_0$	on $0.9V_0$	on ref.: $0.99V_0$, k.o.: $0.9V_0$		on tumour: $0.9V_0$, stroma: $0.99V_0$	
CI threshold number	N_C	off /	off /	off /		on $N_0/2$	Pedigree model (see text)
CIII threshold number migration coefficient	N_C D	off / /	off / /	off / /		on $N_0/2$ 4 D_0 (orientational biased)	
A0 threshold area	A_A	off /	off /	off /	on 250 μm²	off /	

References

1. Ingber, D.E.: Cellular mechanotransduction: putting all the pieces together again. FASEB J. **20**(7), 811–27 (2006)
2. Chen, C.S., Mrksich, M., Huang, S., Whitesides, G.M., Ingber, D.E.: Geometric control of cell life and death. Science **276**, 1425–1428 (1997)
3. Gloushankova, N.A., Alieva, N.A., Krendel, M.F., Bonder, E.M., Feder, H.H., Vasiliev, J.M., Gelfand, I.M.: Cell–cell contact changes the dynamics of lamellar activity in nontransformed epitheliocytes but not in their ras-transformed descendants. Proc. Natl. Acad. Sci. USA **94**, 879–883 (1997)
4. Grant, M.R., Mostov, K.E., Tlsty, T.D., Hunt, C.A.: Simulating properties of in vitro epithelial cell morphogenesis. PLoS Comput. Biol. **6**; 2(10), e129 (2006)
5. Meineke, F.A., Potten, C.S., Loeffler, M.: Cell migration and organisation in the intestinal crypt using a lattice-free model. Cell. Prolif. **34**, 253–266 (2001)
6. Hogeweg, P.: Evolving mechanisms of morphogenesis: on the interplay between differential adhesion and cell differentiation. J. Theor. Biol. **203**, 317–333 (2000)
7. Bauer, A.L., Jackson, T.L., Jiang, Y.: A cell-based model exhibiting branching and anastomosis during tumor-induced angiogenesis. Biophys. J. **92**(9), 3105–3121 (2007)
8. Anderson, A.R.: A hybrid mathematical model of solid tumour invasion: the importance of cell adhesion. Math. Med. Biol. **22**(2), 163–186 (2005)
9. Dormann, S., Deutsch, A.: Modelling of self-organized avascular tumor growth with a hybrid cellular 'automaton. In Silico Biol. **2**(3), 393–406 (2002)
10. Graner, F., Glazier, J.A.: Simulation of biological cell sorting using a two-dimensional extended Potts model. Phys. Rev. Lett. **69**(13), 2013–2016 (1993)
11. Loeffler, M., Potten, C.S., Wichmann, H.E.: Epidermal cell proliferation. Virchows Arch. B **53**, 286–300 (1987)
12. Schaller, G., Meyer-Hermann, M.: Multicellular tumor spheroid in an lattice-free Voronoi-Delaunay cell model. Phys. Rev. E **71**, 051910 (2005)
13. Honda, H., Tanemura, M., Nagai, T.: A three-dimensional vertex dynamics cell model of space-filling polyhedra simulating cell behavior in a cell aggregate. J. Theor. Biol. **226**(4), 439–453 (2004)
14. Brodland, G.W., Veldhuis, J.H.: Computer simulations of mitosis and interdependencies between orientation, cell shape and epithelia reshaping. J. Biomech. **35**, 673–681 (2002)
15. Galle, J., Loeffler, M., Drasdo, D.: Modelling the effect of deregulated proliferation and apoptosis on the growth dynamics of epithelial cell populations in vitro. Biophys. J. **88**(1), 62–75 (2005)
16. Dallon, J., Othmer, H.G.: How cellular movement determines the collective force generated by the Dictyostelium discoideum slug. J. Theor. Biol. **231**(2), 203–222 (2004)

17. Drasdo, D., Höhme, S.: A single-cell-based model of tumor growth in vitro: monolayers and spheroids. Phys. Biol. **2**, 133–147 (2005)
18. Kreft, J.U., Picioreanu, C., Wimpenny, J.W., van Loosdrecht, M.C.: Individual-based modelling of biofilms. Microbiology **147**, 2897–2912 (2001)
19. Palsson, E., Othmer, H.G.: A model for individual and collective cell movement in Dictyostelium discoideum. Proc. Natl. Acad. Sci. USA **97**(19), 10448–10453 (2000)
20. Drasdo, D., Kree, R., McCaskill, J.S.: Monte Carlo approach to tissue-cell populations. Phys. Rev. E **52**(6), 6635–6657 (1995)
21. Schaller, G., Meyer-Hermann, M.: A modelling approach towards epidermal homoeostasis control. J. Theor. Biol. **247**(3), 554–573 (2007)
22. Hoehme, S., Hengstler, J.G., Brulport, M., Schafer, M., Bauer, A., Gebhardt, R., Drasdo, D.: Mathematical modelling of liver regeneration after intoxication with CCl(4). Chem. Biol. Interact. 20 **168**(1), 74–93 (2007)
23. Beyer, T., Meyer-Hermann, M.: Modeling emergent tissue organization involving high-speed migrating cells in a flow equilibrium. Phys. Rev. E: Stat. Nonlin. Soft Matter Phys. **76**(2), 021929 (2007)
24. Galle, J., Sittig, D., Hanisch, I., Wobus, M., Wandel, E., Loeffler, M., Aust, G.: Individual cell-based models of tumor–environment interactions: multiple effects of CD97 on tumor invasion. Am. J. Pathol. **169**(5), 1802–1811 (2006)
25. Engler, A., Bacakova, L., Newman, C., Hategan, A., Griffin, M., Discher, D.: Substrate compliance versus ligand density in cell on gel responses. Biophys. J. **86**, 617–628 (2004)
26. Friedl, P.: Prespecification and plasticity: shifting mechanisms of cell migration. Curr. Opin. Cell Biol. **16**(1), 14–23 (2004)
27. Sahai, E., Marshall, C.J.: Differing modes of tumor cell invasion have distinct requirements for Rho/ROCK signalling and extracellular proteolysis. Nat. Cell Biol. **5**(8), 711–719 (2003)
28. Grunert, S., Jechlinger, M., Beug, H.: Diverse cellular and molecular mechanisms contribute to epithelial plasticity and metastasis. Nat. Rev. Mol. Cell Biol. **4**(8), 657–665 (2003)
29. Hahn, G.M.: State vector description of the proliferation of mammalian cells in tissue culture. I. Exponential growth. Biophys. J. **6**(3), 275–290 (1966)
30. Ingber, D.E.: Tensegrity I. Cell structure and hierarchical systems biology. J. Cell Sci. **116**, 1157–1173 and Tensegrity II. How structural networks influence cellular information processing networks. 1397–1408 (2003)
31. Mahaffy, R.E., Park, S., Gerde, E., Kas, J., Shih, C.K.: Quantitative analysis of the viscoelastic properties of thin regions of fibroblasts using atomic force microscopy. Biophys. J. **86**(3), 1777–1793 (2004)
32. Charras, G.T., Horton, M.A.: Determination of cellular strains by combined atomic force microscopy and finite element modelling. Biophys. J. **83**, 858–879 (2002)
33. Schwarz, U.S., Balaban, N.Q., Riveline, D., Bershadsky, A., Geiger, B., Safran, S.A.: Calculation of forces at focal adhesions from elastic substrate data: the effect of localized force and the need for regularization. Biophys. J. **83**, 1380–1394 (2002)
34. Guck, J., Ananthakrishnan, R., Mahmood, H., Moon, T.J., Cunningham, C.C., Kas, J.: The optical stretcher: a novel laser tool to micromanipulate cells. Biophys. J. **81**(2), 767–784 (2001)
35. Benoit, M., Gabriel, D., Gerisch, G., Gaub, H.E.: Discrete interactions in cell adhesion measured by single-molecule force spectroscopy. Nat. Cell Biol. **2**, 313–317 (2000)
36. Benoit, M., Gaub, H.E.: Measuring cell adhesion forces with the atomic force microscope at the molecular level. Cells Tissues Organs **172**(3), 174–189 (2002)
37. Beysens, D.A., Forgacs, G., Glazier, J.A.: Cell sorting is analogous to phase ordering in fluids. Proc. Natl. Acad. Sci. USA **97**(17), 9467–9471 (2000)
38. Drasdo, D., Hoehme, S., Block, M.: On the role of physics in the growth and pattern formation of multi-cellular systems: what can we learn from individual-cell based models? J. Stat. Phys. **128**, 287–345 (2007)
39. Galle, J., Aust, G., Schaller, G., Beyer, T., Drasdo, D.: Individual cell-based models of the spatial-temporal organization of multicellular systems—achievements and limitations. Cytometry A. **69**(7), 704–710 (2006)
40. Aplin, A.E., Howe, A.K., Juliano, R.L.: Cell adhesion molecules, signal transduction and cell growth. Curr. Opin. Cell Biol. **11**, 737–744 (1999)
41. Mollard, R., Dziadek, M.: A correlation between epithelial proliferation rates, basement membrane component localization patterns, and morphogenetic potential in the embryonic mouse lung. Am. J. Respir. Cell Mol. Biol. **19**(1), 71–82 (1998)

42. Pullan, S., Wilson, J., Metcalfe, A., Edwards, G.M., Goberdhan, N., Tilly, J., Hickman, J.A., Dive, C., Streuli, C.H.: Requirement of basement membrane for the suppression of programmed cell death in mammary epithelium. J. Cell Sci. **109**, 631–642 (1996)
43. Pirone, D.M., Liu, W.F., Ruiz, S.A., Gao, L., Raghavan, S., Lemmon, C.A., Romer, L.H., Chen, C.S.: An inhibitory role for FAK in regulating proliferation: a link between limited adhesion and RhoA-ROCK signaling. J. Cell Biol. **174**(2), 277–288 (2006)
44. DeMali, K.A., Wennerberg, K., Burridge, K.: Integrin signaling to the actin cytoskeleton. Curr. Opin. Cell Biol. **15**(5), 572–582 (2003)
45. Brabletz, T., Spaderna, S., Kolb, J., Hlubek, F., Faller, G., Bruns, C.J., Jung, A., Nentwich, J., Duluc, I., Domon-Dell, C., Kirchner, T., Freund, J.N.: Down-regulation of the homeodomain factor Cdx2 in colorectal cancer by collagen type I: an active role for the tumor environment in malignant tumor progression. Cancer Res. **64**(19), 6973–6977 (2004)
46. Brabletz, T., Jung, A., Reu, S., Porzner, M., Hlubek, F., Kunz-Schughart, L.A., Knuechel, R., Kirchner, T.: Variable beta-catenin expression in colorectal cancers indicates tumor progression driven by the tumor environment. Proc. Natl. Acad. Sci. USA **98**(18), 10356–10361 (2001)
47. Bru, A., Albertos, S., Luis Subiza, J., Garcia-Asenjo, J.L., Bru, I.: The universal dynamics of tumor growth. Biophys. J. **85**(5), 2948–2961 (2003)
48. Helmlinger, G., Netti, P.A., Lichtenbeld, H.C., Melder, R.J., Jain, R.K.: Solid stress inhibits the growth of multicellular tumor spheroids. Nat. Biotechnol. **15**(8), 778–783 (1997)
49. Long, H., Han, H., Yang, B., Wang, Z.: Opposite cell density-dependence between spontaneous and oxidative stress-induced apoptosis in mouse fibroblast L-cells. Cell Physiol. Biochem. **13**(6), 401–414 (2003)
50. Fiore, M., Degrassi, F.: Dimethyl sulfoxide restores contact inhibition-induced growth arrest and inhibits cell density-dependent apoptosis in hamster cells. Exp. Cell Res. **251**(1), 102–110 (1999)
51. Maniotis, A.J., Chen, C.S., Ingber, D.E.: Demonstration of mechanical connections between integrins, cytoskeletal filaments, and nucleoplasm that stabilize nuclear structure. Proc. Natl. Acad. Sci. USA **94**(3), 849–854 (1997)
52. McBeath, R., Pirone, D.M., Nelson, C.M., Bhadriraju, K., Chen, C.S.: Cell shape, cytoskeletal tension, and RhoA regulate stem cell lineage commitment. Dev. Cell **6**(4), 483–495 (2004)
53. Nelson, C.M., Jean, R.P., Tan, J.L., Liu, W.F., Sniadecki, N.J., Spector, A.A., Chen, C.S.: Emergent patterns of growth controlled by multicellular form and mechanics. Proc. Natl. Acad. Sci. U.S.A **102**(33), 11594–11599 (2005)
54. Benaud, C.M., Dickson, R.B.: Adhesion-regulated G1 cell cycle arrest in epithelial cells requires the downregulation of c-Myc. Oncogene **20**(33), 4554–4567 (2001)
55. Ren, X.D., Kiosses, W.B., Sieg, D.J., Otey, C.A., Schlaepfer, D.D., Schwartz, M.A.: Focal adhesion kinase suppresses Rho activity to promote focal adhesion turnover. J. Cell Sci. **113**, 3673–3678 (2000)
56. Steinert, M., Wobus, M., Boltze, C., Schutz, A., Wahlbuhl, M., Hamann, J., Aust, G.: Expression and regulation of CD97 in colorectal carcinoma cell lines and tumor tissues. Am. J. Pathol. **161**(5), 1657–1667 (2002)
57. Friedl, P., Wolf, K.: Tumor-cell invasion and migration: diversity and escape mechanisms. Nat. Rev. Cancer **3**(5), 362–374 (2003)
58. Wang, W., Goswami, S., Sahai, E., Wyckoff, J.B., Segall, J.E., Condeelis, JS.: Tumor cells caught in the act of invading: their strategy for enhanced cell motility. Trends Cell Biol. **15**(3), 138–145 (2005)
59. Chaplain, M.A., Graziano, L., Preziosi, L.: Mathematical modelling of the loss of tissue compression responsiveness and its role in solid tumour development. Math. Med. Biol. **23**(3), 197–229 (2006)
60. Thiery, J.P.: Epithelial–mesenchymal transitions in tumor progression. Nat. Rev. Cancer **2**(6), 442–454 (2002)
61. Brabletz, T., Jung, A., Spaderna, S., Hlubek, F., Kirchner, T.: Opinion: migrating cancer stem cells—an integrated concept of malignant tumour progression. Nat. Rev. Cancer **5**(9), 744–749 (2005)
62. Loeffler, M., Potten, C.S.: Stem cells and cellular pedigrees—a conceptual introduction. In: Potten, C.S. (ed.) Stem Cells, pp. 1–27. Academic Press, London (1997)
63. Quesenberry, P.J., Abedi, M., Aliotta, J., Colvin, G., Demers, D., Dooner, M., Greer, D., Hebert, H., Menon, M.K., Pimentel, J., Paggioli, D.: Stem cell plasticity: an overview. Blood Cells Mol. Dis. **32**(1), 1–4 (2004)
64. Wagers, A.J., Weissman, I.L.: Plasticity of adult stem cells. Cell **116**(5), 639–48 (2004)
65. Loeffler, M., Roeder, I.: Tissue stem cells: definition, plasticity, heterogeneity, self organization and models—a conceptual approach. Cells Tissues Organs **171**(1), 8–26 (2002)

66. Kirkland, M.A.: A phase space model of hemopoiesis and the concept of stem cell renewal. Exp. Hematol. **32**(6), 511–9 (2004)
67. Glauche, I., Cross, M., Loeffler, M., Roeder, I.: Lineage specification of hematopoietic stem cells: mathematical modeling and biological implications. Stem Cells **25**(7), 1791–1799 (2007)
68. Stockholm, D., Benchaouir, R., Picot, J., Rameau, P., Neildez, T.M., Landini, G., Laplace-Builhe, C., Paldi, A.: The origin of phenotypic heterogeneity in a clonal cell population in vitro. PLoS ONE **2**, e394 (2007)
69. Palmqvist, R., Rutegard, J.N., Bozoky, B., Landberg, G., Stenling, R.: Human colorectal cancers with an intact p16/cyclin D1/pRb pathway have up-regulated p16 expression and decreased proliferation in small invasive tumor clusters. Am. J. Pathol. **157**(6), 1947–1953 (2000)
70. Balkwill, F.: Cancer and the chemokine network. Nat. Rev. Cancer **4**(7), 540–550 (2004)
71. Locke, M., Heywood, M., Fawell, S., Mackenzie, I.C.: Retention of intrinsic stem cell hierarchies in carcinoma-derived cell lines. Cancer Res. **65**(19), 8944–8950 (2005)
72. Ichinose, S., Tagami, M., Muneta, T., Sekiya, I.: Morphological examination during in vitro cartilage formation by human mesenchymal stem cells. Cell Tissue Res. **322**(2), 217–226 (2005)
73. Teixeira, A.I., Abrams, G.A., Bertics, P.J., Murphy, C.J., Nealey, P.F.: Epitheilial contact guidance on well-defined micro- and nanostructured substrates. J. Cell Sci. **116**, 1881–1892 (2003)
74. Izaguirre, J.A., Chaturvedi, R., Huang, C., Cickovski, T., Coffland, J., Thomas, G., Forgacs, G., Alber, M., Hentschel, G., Newman, S.A., Glazier, J.A.: CompuCell, a multi-model framework for simulation of morphogenesis. Bioinformatics **20**(7), 1129–1137 (2004)
75. Teller, I.C., Beaulieu, J.F.: Interactions between laminin and epithelial cells in intestinal health and disease. Exp. Rev. Mol. Med. **28**(09), 1–16 (2001)
76. Preston, S.L., Wong, W.M., Chan, A.O., Poulsom, R., Jeffery, R., Goodlad, R.A., Mandir, N., Elia, G., Novelli, M., Bodmer, W.F., Tomlinson, I.P., Wright, N.A.: Bottom-up histogenesis of colorectal adenomas: origin in the monocryptal adenoma and initial expansion by crypt fission. Cancer Res. **63**(13), 3819–3825 (2003)
77. Roeder, I., Glauche, I.: Towards an understanding of lineage specification in hematopoietic stem cells: a mathematical model for the interaction of transcription factors GATA-1 and PU.1. J. Theor. Biol. **241**(4), 852–865 (2006)
78. Pribyl, M., Muratov, C.B., Shvartsman, S.Y.: Discrete models of autocrine cell communication in epithelial layers. Biophys. J. **84**(6), 3624–3635 (2003)
79. Roose, T., Chapman, S.J., Maini, P.K.: Mathematical models of avascular cancer. SIAM Rev. **49**(2), 179–208 (2007)
80. Frisch, T., Thoumine, O.: Predicting the kinetics of cell spreading. Biomechanics **35**(8), 1137–1141 (2002)
81. Grossmann, J., Walther, K., Artinger, M., Kiessling, S., Schölmerich, J.: Apoptotic signaling during initiation of detachment-induced apoptosis ("anoikis") of primary human intestinal epithelial cells. Cell Growth Differ. **12**(3), 147–155 (2001)